

Neutralino Relic Density with a Cosmological Constant confronts Electroweak Precision Measurements

A. B. Lahanas¹, D. V. Nanopoulos² and V. C. Spanos¹

¹ *University of Athens, Physics Department, Nuclear and Particle Physics Section,
GR-15771 Athens, Greece*

² *Department of Physics, Texas A & M University, College Station, TX 77843-4242,
USA, Astroparticle Physics Group, Houston Advanced Research Center (HARC),
Mitchell Campus, Woodlands, TX 77381, USA, and
Academy of Athens, Chair of Theoretical Physics, Division of Natural Sciences,
28 Panepistimiou Avenue, Athens 10679, Greece*

Abstract

We discuss the relic density of the lightest of the supersymmetric particles (LSP) in view of new cosmological data, which favour the concept of an accelerating Universe with a non-vanishing cosmological constant. The new bound on the Cold Dark Matter density, $\Omega_{\text{CDM}} h_0^2 \lesssim 0.22$, puts stringent constraints on supersymmetry preferring low supersymmetry breaking scales, in sharp contrast to electroweak precision measurements favouring large supersymmetry breaking scales. Supersymmetric predictions are in agreement with cosmological data and electroweak precision data in the window of the parameter space: $m_0 < 200$ GeV, $300 \text{ GeV} < M_{1/2} < 400$ GeV, putting bounds on sparticle masses, which may be evaded if $m_{\text{LSP}} < m_{\tilde{\tau}_R} \lesssim 1.2 m_{\text{LSP}}$.

Recent observations of type Ia supernovae (SNIa) put new constraints on the cosmological parameters. The data favour an almost *flat* and *accelerating* Universe, where the acceleration mainly is driven by a *non-vanishing cosmological constant*.

There is a growing consensus that the anisotropy of the Cosmic Background Radiation (CBR) offers the best way to determine the curvature of the Universe and hence the total matter-energy density Ω_0 [1]. The data are consistent with a flat Universe, since $\Omega_0 = 1.0 \pm 0.2$ [1,2], and the radiation content of the matter-energy density, that is contribution coming from CBR and/or ultra relativistic neutrinos, is very small. Therefore the present matter-energy density can be decomposed basically into two components: the matter density Ω_M and the vacuum energy Ω_Λ :

$$\Omega_0 = \Omega_M + \Omega_\Lambda . \quad (1)$$

There is supporting evidence, coming from many independent astrophysical observations, that the matter density weighs $\Omega_M = 0.4 \pm 0.1$. Recently two groups, the Supernova Cosmology Project [3] and the High- z Supernova Search Team [4], using different methods of analysis, each found evidence for accelerated expansion, driven by a vacuum energy contribution:

$$\Omega_\Lambda = \frac{4}{3}\Omega_M + \frac{1}{3} \pm \frac{1}{6} . \quad (2)$$

So, for $\Omega_M = 0.4 \pm 0.1$ this relation implies that the vacuum energy is non-vanishing, $\Omega_\Lambda = 0.85 \pm 0.2$, value which is compatible with a flat Universe, as the anisotropy of CBR measurements indicate. Taking into account the fact that the baryonic contribution to the matter density is small, $\Omega_B = 0.05 \pm 0.005$, the values for matter energy density Ω_M result to a Cold Dark Matter (CDM) density $\Omega_{\text{CDM}} \simeq 0.35 \pm 0.1$, which combined with more recent measurements [1,5] of the scaled Hubble parameter $h_0 = 0.65 \pm 0.05$, result to small CDM relic densities:

$$\Omega_{\text{CDM}} h_0^2 \simeq 0.15 \pm 0.07 . \quad (3)$$

Such stringent bounds for the CDM relic density do affect supersymmetric predictions and can severely lower the limits of the effective supersymmetry breaking scale and hence the masses of the supersymmetric particles, as first emphasized in Ref. [6]. The CDM relic density with non-vanishing cosmological constant in the framework of the Minimal

Supersymmetric Standard Model (MSSM) has been the subject of Ref. [7]. Using the recent cosmological data, gauge fermions are predicted to be within LHC reach.

It is perhaps worth pointing out that while electroweak (EW) precision data are in perfect agreement with Standard Model (SM) predictions, and hence in agreement too with supersymmetric models characterized by a large supersymmetry breaking scale M_{SUSY} [8], the data on $\Omega_{\text{CDM}} h_0^2$ push M_{SUSY} to the opposite direction favouring small values of M_{SUSY} . Therefore EW precision data may not reconcile with the assumption that the lightest supersymmetric particle (LSP or $\tilde{\chi}$), is a candidate for CDM.

In R -parity conserving supersymmetric theories the LSP is stable, and for most of supersymmetric models is the lightest neutralino, which is a good candidate for the CDM particle [9]. Many authors [10–25] have calculated the relic neutralino density. In the early works, only the most important neutralino annihilation channels were considered, but later works [20,21] included all annihilation channels. Also more refined calculations of thermal averages of cross sections were employed, which took into account threshold effects and integration over Breit–Wigner poles [26,27].

Our study in this letter is based on the constrained supergravity (SUGRA) scenario, assuming universal boundary conditions for the soft breaking parameters at the unification scale M_{GUT}^1 . It is also assumed that the EW symmetry is radiatively broken [28]. Therefore the arbitrary parameters are: m_0 , $M_{1/2}$, A_0 and $\tan\beta$. The absolute value of μ is determined from the minimization conditions of the one-loop corrected effective potential. These also determine the Higgs mixing parameter m_3^2 . The sign of μ is undetermined in this procedure and in our analysis both signs of μ are considered. Therefore in this scheme the μ value as well as $m_3^2 \equiv B\mu$ are not inputs.

The Boltzmann transport equation for the neutralino number density is:

$$\frac{dn}{dt} = -3Hn - \langle\sigma v_{rel}\rangle (n^2(T) - n_0^2(T)), \quad (4)$$

where n is the number of $\tilde{\chi}$'s per unit volume, n_0 is their density in thermal equilibrium and H is the expansion rate of the Universe. Using the fact that the total entropy $S = h T^3 R^3$ is conserved and defining the quantity $q(x) \equiv \frac{n(T)}{T^3 h(T)}$ with $x \equiv T/m_{\tilde{\chi}}$, this

¹We allow however for small deviations from the gauge coupling unification scenario. In this case the value of the strong coupling constant at the unification scale, defined as the point where the couplings α_1 and α_2 meet, is different from $\alpha_{1,2}$.

differential equation can be cast into a form suitable for numerical manipulations [11]:

$$\frac{dq}{dx} = \lambda(x) (q^2 - q_0^2), \quad (5)$$

where

$$\lambda(x) \equiv \left(\frac{4\pi^3}{45} G_N \right)^{-1/2} \frac{m_{\tilde{\chi}}}{\sqrt{g(T)}} \left(h(T) + \frac{m_{\tilde{\chi}}}{3} h'(T) \right) \langle \sigma v_{rel} \rangle. \quad (6)$$

The functions $g(T)$ and $h(T)$ appearing in the equation above, are the effective energy and entropy degrees of freedom respectively, and they determine the Universe energy and entropy density through the relations:

$$\rho(T) = \frac{\pi^2}{30} T^4 g(T), \quad s(T) = \frac{2\pi^2}{45} T^3 h(T). \quad (7)$$

Solving Eq. (5) we obtain the $q(x_0)$, where $x_0 \equiv T_0/m_{\tilde{\chi}}$ corresponds to today's Universe temperature $T_0 \approx 2.7$ K. Using that $q \equiv \frac{n(T)}{T^3 h(T)}$, $\Omega_{\tilde{\chi}} = \frac{\rho_{\tilde{\chi}}}{\rho_{crit}}$ and $\rho_{crit} = \frac{3H_0^2}{8\pi G_N}$, we determine the present value of neutralino relic density $\Omega_{\tilde{\chi}} h_0^2$ from the equation:

$$\Omega_{\tilde{\chi}} h_0^2 = \frac{8\pi}{3} T_0^3 G_N m_{\tilde{\chi}} h(x_0) q(x_0) (100 \text{ km sec}^{-1} \text{ Mpc}^{-1})^{-2}. \quad (8)$$

Before solving the Boltzmann equation we need to calculate the effective degrees of freedom functions $g(T)$ and $h(T)$, as well as the thermally averaged cross section $\langle \sigma v_{rel} \rangle$, which enter into Eq. (5). Regarding the calculation of the functions $g(T)$ and $h(T)$, the content of the particles in equilibrium is different depending on the temperature T . In our analyses we use the expressions for $g(T)$, $h(T)$ as given in Ref. [19]. Next we turn to the calculation of $\langle \sigma v_{rel} \rangle$. At this point we follow Ref. [20] and express the non-relativistic cross sections for the various annihilation processes $\tilde{\chi} \tilde{\chi} \rightarrow XY$, in terms of helicity amplitudes. We follow the standard treatment and ignore contributions of all channels, which are forbidden at zero relative velocity v_{rel} of the two annihilating $\tilde{\chi}$'s. This approximation is not expected to invalidate significantly our results. So we consider only the contributions of channels with non-supersymmetric particles in the final state:

$$q\bar{q}, \bar{l}l, W^+W^-, ZZ, ZH, Zh, ZA, W^\pm H^\mp, HH, hh, Hh, AA, HA, hA, H^+H^-.$$

q and l denote quarks and leptons respectively, while H , h , A and H^\pm denote the heavy, light, pseudoscalar and charged Higgses respectively. In our analysis we have not studied neutralino–stau coannihilation effects [15,24,26], which if included can lower the

values of the neutralino relic density. Although important, coannihilation processes are of relevance for values of the parameters for which $m_{\tilde{\chi}} < m_{\tilde{\tau}_R} \lesssim 1.2 m_{\tilde{\chi}}$, that is near the edge where $\tilde{\chi}$ and $\tilde{\tau}_R$ are almost degenerate in mass.

It is well known that the non-relativistic expansion in the relative velocity v_{rel} breaks down near thresholds or poles of the cross sections, and in these cases, results based on this expansion are unreliable. We locate the points of the parameter space of the MSSM, which result to pole and/or thresholds of the cross section, using “near pole” and “near threshold” criteria. The comparison of our results with those of other studies [17, 21], which treat the problem of poles and thresholds in a more accurate manner, shows that they are in striking agreement. This occurs, at least, in regions of the parameter space of MSSM where this comparison is feasible.

Knowing $\langle \sigma v_{rel} \rangle$, from the procedure outlined previously, and by calculating the functions $g(T)$, $h(T)$, $h'(T)$ we can have the prefactor $\lambda(x)$ appearing in Eq. (5). At high temperatures, or same large values of $x = T/m_{\tilde{\chi}}$ above the freeze-out temperature, the function $q(x)$ approaches its equilibrium value $q_0(x)$ (see Eq. 5). A convenient and accurate method for solving the Boltzmann equation is the WKB approximation employed in Ref. [19]. As far as the scanning of the parameter space of the MSSM is concerned, we exclude points that are theoretically forbidden, such as those leading to breaking of lepton and/or color number, or points for which Landau poles are developed and so on. We also exclude points for which the LSP is not a neutralino, as well as points of the parameter space for which violation of the experimental bounds on sparticle masses is encountered. We use the bounds which are listed in Ref. [29]. From these bounds we have found that the chargino mass bound turns out to be the most stringent one. Details on our calculation will be published elsewhere [30].

Before embarking to discuss our physics results we should stress that in our scheme we have not made any approximation concerning the masses or couplings of sectors which are rather involved such as neutralini for instance, which are crucial for our analysis. Therefore we do not only consider regions of the parameter space in which the LSP is purely \tilde{B} (bino) or purely a Higgsino, but also regions where in general the LSP happens to be an admixture of the four available degrees of freedom².

² The case of a Higgsino-like LSP has been pursued in Refs. [23, 25], where the dominant radiative corrections to neutralino masses are considered. Analogous corrections to couplings of Higgsino-like

For large values of the LSP mass many channels are open, but for small values ($m_{\tilde{\chi}} < 40$ GeV) only channels with fermions, with the exclusion of top quark, in the final state are contributing. In these processes the exchanged particles can be either a Z -boson and a Higgs in the s -channel, as well as a sfermion \tilde{f} in the t -channel. Higgs exchanges are suppressed by their small couplings to light fermions, and sfermion exchanges are suppressed when their masses are large. Then the only term surviving, even for large values of squark or slepton masses, is the Z -boson exchange. However in the parameter region where the LSP is a bino, this is not coupled to the Z -boson resulting to very small cross sections enhancing dramatically the LSP relic density. Therefore in considerations in which the LSP is a light bino³, large squark or slepton masses are inevitably excluded, since they lead to large relic densities. If one relaxes this assumption and considers regions of the parameter space in which the LSP is light but is not purely bino, heavy squarks or sleptons may be allowed. We shall return to this later. Therefore the possibility for heavy \tilde{q} or \tilde{l} in the sparticle spectrum still exists, at the expense of having a light LSP and one of the chargino states.

We have scanned the parameter space for values of m_0 , $M_{1/2}$, A_0 up to 1 TeV and $\tan\beta$ from around 1.8 to 35 for both positive and negative values of μ . The top quark mass is taken 175 GeV. In Figure 1, we display a representative output in the $(M_{1/2}, m_0)$ plane for fixed values of A_0 and $\tan\beta$. Although in the displayed figure only values for $\mu > 0$ are presented, in our analysis both signs of μ have been considered. In the displayed figures A_0 takes the values $A_0 = 0$ and $\tan\beta = 5, 20$. The five different grey tone regions met as we move from bottom left to right up, correspond to regions in which $\Omega_{\tilde{\chi}} h_0^2$ takes values in the intervals $0.00 - 0.08$, $0.08 - 0.22$, $0.22 - 0.35$, $0.35 - 0.60$ and $0.60 - 1.00$ respectively⁴.

In the blanc area covering the right up region, the relic density is found to be larger than unity. In the area to the left of the figure, the chargino mass bound is violated. Whenever a cross appears it designates that we are near either a pole or a threshold according to the criteria given previously. In these cases the approximations used are

neutralinos to Z and Higgs bosons are important and can increase the relic density by a factor of 5, in regions of parameter space where LSP is a high purity Higgsino state [23].

³ This happens when $|\mu| \gg M_W$, with M_1 small $\approx M_W$.

⁴These regions have been chosen in accord with the new bounds on $\Omega_{\tilde{\chi}} h_0^2$ quoted in the introduction, and less stringent bounds on the same quantity which have been previously used in other works.

untrustworthy and no safe conclusions can be drawn. For low values of $M_{1/2}$ crosses correspond to mainly poles, which are either Z -boson or light Higgs, while for higher values, where LSP is heavier and hence new channels are open, these correspond to thresholds. For $M_{1/2} \approx 110$ GeV (≈ 90 GeV for $\mu < 0$) the lightest of the chargini has a mass close to its experimental lower limit. This bound is violated for all points $M_{1/2} \leq 100$ GeV. The dark area at the bottom part of the figure, which occurs for low values of m_0 , $m_0 \leq 100$ GeV, is excluded since it mainly includes points for which the LSP is not a neutralino. In a lesser extend some of these correspond to points, which are theoretically excluded in the sense that either radiative breaking of the EW symmetry does not occur and/or other unwanted minima, breaking color or lepton number, are developed.

For fixed $M_{1/2} > 150$ GeV the relic density $\Omega_{\tilde{\chi}} h_0^2$ increases as m_0 increases, due to the fact that cross sections involving sfermion exchanges decrease. Thus the area filled by the points corresponding to $\Omega_{\tilde{\chi}} h_0^2 < 0.22$ concentrates to the left bottom of the figure ($m_0 < 200$ GeV). Also for fixed $m_0 < 250$ GeV the number of points for which $\Omega_{\tilde{\chi}} h_0^2 < 0.22$ decreases as $M_{1/2}$ increases since an increase in $M_{1/2}$, enlarges squark and slepton masses as well yielding smaller cross sections. If $M_{1/2}$ is further increased, for fixed m_0 , the LSP will eventually cease to be a neutralino⁵. This picture changes for small values $M_{1/2} \approx 100$ GeV, (see for instance the first of Figures 1) in which case small values of $\Omega_{\tilde{\chi}} h_0^2 < 0.22$ can occur even for large values of the parameter $m_0 > 300$ GeV. This happens because the LSP is not a bino in this region and Z -boson exchanges contribute substantially to the annihilation of LSP's into light fermions, as explained previously. Actually in this region $|\mu|$ is not much larger than the EW scale M_W and the LSP, although mostly bino, contains a sizeable portion of H_1 Higgsino, leading to sizeable cross sections.

Therefore the neutralino relic density does not exclude heavy squark or slepton states, as long as LSP is light, containing substantial mixture of Higgsinos⁶. In all cases where this takes place, the LSP turns out to be light $m_{\tilde{\chi}} \approx 40$ GeV or smaller and thus the only

⁵The region for which the LSP is not a neutralino depends rather strongly on the parameters A_0 and $\tan\beta$. Actually for large values of these parameters the light stau becomes lighter than the neutralinos.

⁶ These corridors of low $M_{1/2}$ and large m_0 values have been also presented in Ref. [21]. The figures of that reference displaying values of relic density in the $(M_{1/2}, m_0)$ plane are in remarkable agreement with our corresponding figures.

open channels are those involving light fermions in the final state. Then the annihilation of LSP's into neutrinos for instance, a channel which is always open, proceeds via the exchange of a Z -boson which is non-vanishing and dominates the reaction when m_0 is sufficiently large, due to the heaviness of sfermions. This puts a lower bound on $\langle\sigma v_{rel}\rangle$ and hence an upper bound on $\Omega_{\tilde{\chi}} h_0^2$, which can be lower than 0.22 consistent with the upper experimental limits quoted in the introduction. On these grounds one would expect that by increasing m_0 , while keeping $M_{1/2} \approx 100$ GeV fixed, the relic density stays below its upper experimental limit. However, with the exception of a few cases, this is not so in all cases studied. In some of the cases, beyond a certain point along the m_0 axis, $\Omega_{\tilde{\chi}} h_0^2$ exceeds the value 0.22 and starts increasing monotonically. This is due to the fact that the parameter $|\mu|$ gets large again making LSP moving towards the bino region. In this case cross sections are suppressed, since the coupling of LSP to Z -boson are negligible and sfermions are quite massive, and therefore the relic density is enhanced. As a further remark, we have to point out that the cosmologically allowed corridors of low $M_{1/2}$ and high m_0 values, which we have just discussed, are almost ruled out in view of newer data on chargino masses [31], which push up the lower bound for the soft gaugino mass $M_{1/2}$ to about 130 GeV.

It is seen from Figures 1 that as $\tan\beta$ increases the points for which the LSP is not a neutralino increase in number. As said before, this is due to the fact that by increasing $\tan\beta$ the stau sfermion $\tilde{\tau}_R$ becomes lighter, since masses of the sfermions of the third generation have a rather strong dependence on $\tan\beta$. For exactly the same reasons this is also the case when we increase the soft parameter A_0 . For lack of space we do not display this case [30].

In Figures 2,3,4 we plot representative outputs of the relic density as function of one of the parameters m_0 , $M_{1/2}$, A_0 and $\tan\beta$ keeping the other three fixed. In Figure 2 the relic density is plotted against m_0 ; the lines shown correspond to different values for $M_{1/2}$. Notice that at the point where each line starts the mass of the LSP is equal to that of $\tilde{\tau}_R$. From this figure it is obvious the tendency to get acceptable values for the relic density, as long as m_0 and $M_{1/2}$ are kept light. Also obvious is the fact that larger values of m_0 are obtained for large values of $\tan\beta$.

In Figure 3 the relic density is shown as function of the soft parameter $M_{1/2}$. Low

values of $M_{1/2} < 120$ GeV (110 GeV) for $\tan\beta = 5$ (20) are not allowed because of the chargino mass bound. It is clearly seen that low values of $M_{1/2}$ are preferred. The upper bounds on $M_{1/2}$, which are compatible with the cosmological data, are higher for low m_0 and large $\tan\beta$. In this figure crosses denote location of poles or thresholds.

In the first of Figures 4 we display the relic density as a function of A_0 . We have chosen $\tan\beta = 20$. Lowering the value of $\tan\beta$, keeping $m_0, M_{1/2}$ fixed, the curves shown move upwards away from the shaded stripe, which is cosmologically accepted. In the second figure $\Omega_{\tilde{\chi}} h_0^2$ is plotted as a function of $\tan\beta$. One immediately notices the tendency for the relic density to decrease as $\tan\beta$ gets large.

Scattered plots of LSP relic density are shown in Figure 5. The sample consists of 4000 random points that cover the most interesting part of the parameter space, which is within the limits: $1.8 < \tan\beta < 40$, $M_{1/2} < 1$ TeV, $|A_0| < 500$ GeV and $m_0 < 500$ GeV⁷. From the given sample only those points which lead to relics less than 1.5 are shown in the figure. The experimental bounds discussed before, restrict by about 40% the values of the allowed points. Low values of $M_{1/2}$ less than about 100 GeV are experimentally forbidden by chargino searches. The points shown are striken by a cross (\times) when $m_0 < 100$ GeV, by a plus (+) when 100 GeV $< m_0 < 200$ GeV and by a diamond (\diamond) when m_0 exceeds 200 GeV. It is obvious the tendency to have $M_{1/2} < 400$ GeV in the cosmologically interesting domain which lies in the stripe between the two lines at 0.08 and 0.22. Actually except for a few isolated cases, all allowed points are accumulated between $M_{1/2} \approx 110 - 380$ GeV. Note that the values of the parameter m_0 in the allowed area are restricted to mainly $m_0 < 200$ GeV (crosses or pluses). Only a few points with large values $m_0 > 200$ GeV are consistent with the recent cosmological data.

EW precision data are in perfect agreement with the SM and therefore with supersymmetric extensions of it which are characterised by a large M_{SUSY} . In fact overall fits to the EW precision data show a preference towards large values of M_{SUSY} , in which case better fits (lower χ^2) are obtained [8]. In the constrained MSSM lower bounds on $M_{1/2}$ can be established from the experimental value of the effective weak mixing angle $\sin^2\theta_{\text{eff}}$, measured in SLC and LEP experiments. If the combined SLC and LEP data are

⁷ Higher values for m_0 are of relevance only for $M_{1/2} \approx 100$ GeV. Such low values for $M_{1/2}$ are almost ruled out by recent data. Also since $\Omega_{\tilde{\chi}} h_0^2$ does not depend strongly on A_0 for $M_{1/2} > 100$ GeV, as it can be realised from the first of the Figures 4, it suffices to focus on values $|A_0| < 500$ GeV.

used, $M_{1/2}$ is restricted to be larger than about 300 GeV (see Dedes *et. al.* in Ref. [8]⁸). This lower bound on $M_{1/2}$ can be further increased by about 200 GeV, if in addition gauge coupling unification is assumed⁹.

Following the previous discussion, in Figure 5 we have shaded in grey the region which is consistent with EW precision data. This starts at about 300 GeV and progressively becomes darker as we move to larger $M_{1/2}$ values, where the SM limit is attained and better agreement with experimental data is obtained. We observe that only a few points, the majority of them being very close to 400 GeV, are compatible with both astrophysical and EW precision measurements. The values of $M_{1/2}$ and m_0 for which theoretical predictions agree with both data, are constrained within the regions $300 \text{ GeV} < M_{1/2} < 400 \text{ GeV}$ and $m_0 < 200 \text{ GeV}$. Performing a more refined scanning in the parameter space with values of $M_{1/2}$, m_0 in the aforementioned range and varying the other two in the range $1.8 < \tan\beta < 40$, $|A_0| < 1 \text{ TeV}$, we have found the following lower and upper bounds on the masses of the LSP, the lighter of charginos, staus, stops and the light scalar Higgs:

$$\begin{aligned}
m_{\text{LSP}} & : 113 \text{ GeV} - 149 \text{ GeV} , \\
m_{\tilde{C}} & : 209 \text{ GeV} - 278 \text{ GeV} , \\
m_{\tilde{\tau}_R} & : 118 \text{ GeV} - 168 \text{ GeV} , \\
m_{\tilde{t}_1} & : 390 \text{ GeV} - 720 \text{ GeV} , \\
m_{h_0} & : 76 \text{ GeV} - 122 \text{ GeV} .
\end{aligned}$$

These refer to the case $\mu > 0$. Analogous bounds are found for $\mu < 0$. With the exception of the Higgs lower bound, which is increased by about 20 GeV, the bounds for the remaining sparticles in the $\mu < 0$ case are almost unchanged. Since we have neglected coannihilation effects, the conclusions reached are actually valid outside the stripe $m_{\tilde{\chi}} < m_{\tilde{\tau}_R} \lesssim 1.2 m_{\tilde{\chi}}$. Inside this band $\tilde{\chi} - \tilde{\tau}$ coannihilations dominate the cross sections, decreasing $\tilde{\chi}$ relic densities leaving corridors of opportunity to high $M_{1/2}$ and m_0 values as emphasized in other studies [24].

⁸SLC data alone leave more freedom by allowing for lower $M_{1/2}$ values. On the contrary LEP data alone prefer large values of $M_{1/2}$.

⁹However since this result depends sensitively on possible existence of High Energy thresholds we do not impose such a strong lower bound on $M_{1/2}$ values.

In conclusion we can say that the new stringent bound on the matter relic density $\Omega_{\tilde{\chi}} h_0^2 \lesssim 0.22$ extracted from recent data, prefer low supersymmetry breaking scales and hence a light sparticle spectrum, provided $m_{\tilde{\tau}_R} > 1.2 m_{\tilde{\chi}}$. This behaviour is exactly the opposite of what happens in the EW precision measurements physics. Reconciling LEP/SLC data with recent cosmological measurements restricts the parameters of the constrained minimal supersymmetry, yielding values of some of the sparticle masses not far away from their lower experimental limits.

Acknowledgments

A.B.L. acknowledges support from ERBFMRXCT-960090 TMR programme and D.V.N. by D.O.E. grant DE-FG03-95-ER-40917. V.C.S. acknowledges an enlightening discussion with D. Schwarz.

References

- [1] “Cosmological Parameters”, M. Turner, to be published in the “Particle Physics and Early Universe” (Cosmo ’98), Monterey CA–US, astro-ph/9904051.
- [2] C. Lineweaver, *Astrophys. J. Lett.* 69 (1998) 505.
- [3] S. Perlmutter *et. al.*, *Astrophys. J.*, in press, astro-ph/9812133.
- [4] A. Riess *et. al.*, *Astron. J.* 116 (1998) 1009; B. Schmidt *et. al.*, *Astrophys. J.* 46 (1998) 507.
- [5] B. Chaboyer, *Phys. Rep.* in press, astro-ph/9808200; W. Freedman, *Physica Scripta* in press.
- [6] J.L. Lopez and D.V. Nanopoulos, *Mod. Phys. Lett.* A9 (1994) 2755.
- [7] J. Wells, *Phys. Lett.* B443 (1998) 196.
- [8] G.A. Altarelli, R. Barbieri and F. Caravaglios, *Int. J. Mod. Phys.* A13 (1998) 103; P. Chankowski and S. Pokorski, “Perspectives in Supersymmetry” edited by G.L. Kane, World Scientific 1997, hep-ph/9707497; J. Bagger, K. Matchev, D. Pierce and R. Zhang, *Nucl. Phys.* B491 (1997) 3; J. Erler and D. Pierce, *Nucl. Phys.* B526 (1998) 53; A. Dedes, A.B. Lahanas and K. Tamvakis, *Phys. Rev.* D59 (1999) 015019.
- [9] S. Weinberg, *Phys. Rev. Lett.* 50 (1983) 387; H. Goldberg, *Phys. Rev. Lett.* 50 (1983) 1419; L.M. Krauss, *Nucl. Phys.* B227 (1983) 556; J. Ellis, J. Hagelin, D.V. Nanopoulos and M. Srednicki, *Phys. Lett.* 127B (1983) 233.
- [10] J. Ellis, J. Hagelin, D.V. Nanopoulos, K. Olive and M. Srednicki, *Nucl. Phys.* B283 (1984) 453; J. Ellis, J. Hagelin and D.V. Nanopoulos, *Phys. Lett.* 159B (1985) 26; J.S. Hagelin, G.L. Kane and S. Raby, *Nucl. Phys.* B241 (1984) 638; L.E. Ibañez, *Phys. Lett.* B137 (1984) 160.
- [11] M. Srednicki, R. Watkins and K.A. Olive, *Nucl. Phys.* B310 (1988) 693.
- [12] K. Griest, *Phys. Rev.* D38 (1988) 2357; K. Griest, *Phys. Rev.* D38 (1988) 2357 [Erratum: D39 (1989) 3802].

- [13] R. Barbieri, M. Friegeni and G.F. Giudice, Nucl. Phys. B313 (1989) 715; J. Ellis, L. Roszkowski and Z. Lalak, Phys. Lett. B245 (1990) 545; J. Ellis, D.V. Nanopoulos, L. Roszkowski and D.N. Schramm, Phys. Lett. B245 (1990) 251; L. Roszkowski Phys. Lett. B252 (1990) 471; Phys. Lett. B262 (1991) 59; J. Ellis and L. Roszkowski, Phys. Lett. B283 (1992) 252; L. Roszkowski and R. Roberts, Phys. Lett. B309 (1993) 329; G.L. Kane, C. Kolda, L. Roszkowski and J.D. Wells, Phys. Rev. D49 (1994) 6173; E. Diehl, G.L. Kane, C. Kolda and J.D. Wells, Phys. Rev. D52 (1995) 4223.
- [14] K.A. Olive and M. Srednicki, Phys. Lett. B230 (1989) 78; Nucl. Phys. B355 (1991) 208; K. Griest, M. Kamionkowski and M.S. Turner, Phys. Rev. D41 (1990) 3565; J. McDonald, K.A. Olive and M. Srednicki, Phys. Lett. B283 (1992) 80; S. Mizuta, D. Ng and M. Yamaguchi, Phys. Lett. B300 (1993) 96.
- [15] S. Mizuta and M. Yamaguchi, Phys. Lett. B298 (1993) 120.
- [16] J. Ellis and F. Zwirner, Nucl. Phys. B338 (1990) 317; M.M. Nojiri, Phys. Lett. B261 (1991) 76; J.L. Lopez, D.V. Nanopoulos and K. Yuan, Phys. Lett. B267 (1991) 219; J.L. Lopez, D.V. Nanopoulos, H. Pois and K. Yuan, Phys. Lett. B273 (1991) 423; M. Kawasaki and S. Mizuta, Phys. Rev. D46 (1992) 1634; S. Kelley, J.L. Lopez, D.V. Nanopoulos, H. Pois and K. Yuan, Phys. Rev. D47 (1993) 2461.
- [17] J.L. Lopez, D.V. Nanopoulos and K. Yuan, Phys. Rev. D48 (1993) 2766.
- [18] R. Arnowitt and P. Nath, Phys. Lett. B299 (1993) 58 [Erratum: B307 (1993) 403]; Phys. Rev. Lett. 70 (1993) 3696; Phys. Rev. D54 (1996) 2374; M. Drees and A. Yamada, Phys. Rev. D53 (1996) 1586; J. Ellis, T. Falk, K.A. Olive and M. Schmitt, Phys. Lett. B388 (1996) 97.
- [19] J.L. Lopez, D.V. Nanopoulos and K. Yuan, Nucl. Phys. B370 (1992) 445.
- [20] M. Drees and M.M. Nojiri, Phys. Rev. D47 (1993) 376.
- [21] H. Baer and M. Brhlik, Phys. Rev. D53 (1996) 597; V. Barger and C. Kao, Phys. Rev. D57 (1998) 3131.

- [22] For recent review, see G. Jungman, M. Kamionkowski and K. Griest, Phys. Rep. 267 (1996) 195.
- [23] M. Drees, M.M. Nojiri, D.P. Roy and Y. Yamada, Phys. Rev. B56 (1997) 276.
- [24] J. Ellis, T. Falk and K.A. Olive, Phys. Lett. B413 (1998) 355; J. Ellis, T. Falk, K.A. Olive and M. Srednicki, hep-ph/9905481.
- [25] J. Ellis, T. Falk, G. Ganis and K.A. Olive, Phys. Rev. B58 (1998) 095002.
- [26] K. Griest and D. Seckel, Phys. Rev. D43 (1991) 3191.
- [27] P. Gondolo and G. Gelmini, Nucl. Phys. B360 (1991) 145.
- [28] For review see A.B. Lahanas and D.V. Nanopoulos, Phys. Rep. 145 (1987) 1.
- [29] Particle Data Group, Euro. Phys. J. C3 (1998) 1.
- [30] A.B. Lahanas, D.V. Nanopoulos and V.C. Spanos, to appear.
- [31] “Search for charginos and neutralinos in e^+e^- collisions at centre-of-mass energies near 183 GeV and constraints on the MSSM parameter space”, ALEPH coll., CERN-EP/99-014; “Search for chargino and neutralino production at $\sqrt{s} = 181 - 184$ GeV at LEP”, OPAL coll., CERN-EP/98-136, hep-ex/9809031.

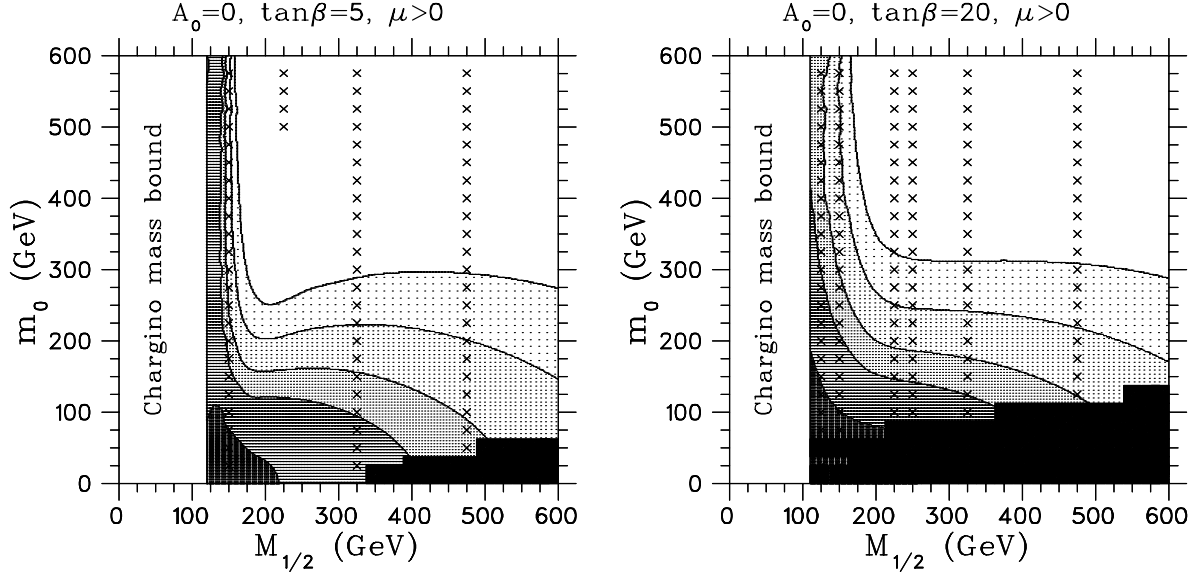


Figure 1: The LSP relic density $\Omega_{\tilde{\chi}} h_0^2$ in the $(m_0, M_{1/2})$ plane for given values of A_0 , $\tan\beta$ and sign of μ . Grey tone regions, from darker to lighter, designate areas in which the LSP relic density takes values in the intervals: $0.00 - 0.08$, $0.08 - 0.22$, $0.22 - 0.35$, $0.35 - 0.60$ and $0.60 - 1.00$ respectively. In the blanc area $\Omega_{\tilde{\chi}} h_0^2 > 1.0$. The dark area corresponds to points for which the LSP is not a neutralino. The area which is excluded by chargino searches, $m_{\tilde{C}} > 66$ GeV, is also shown. Crosses denote points for which thresholds or poles are encountered.

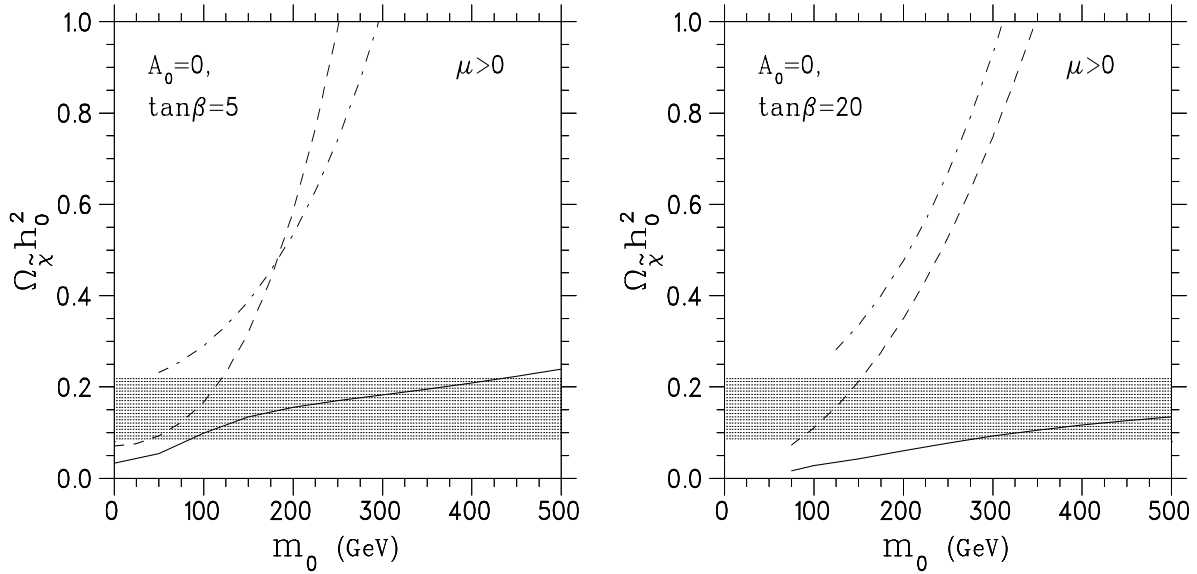


Figure 2: The relic density as function of m_0 for fixed values of A_0 , $\tan\beta$ shown in the figure. The solid line corresponds to $M_{1/2} = 120$ GeV (110 GeV) for $\tan\beta = 5$ (20), the lowest allowed values by the chargino searches (see Figure 1). The dashed and dot-dashed lines correspond to $M_{1/2} = 200$ and 400 GeV respectively. The grey area corresponds to $\Omega_{\tilde{\chi}} h_0^2 = 0.15 \pm 0.07$.

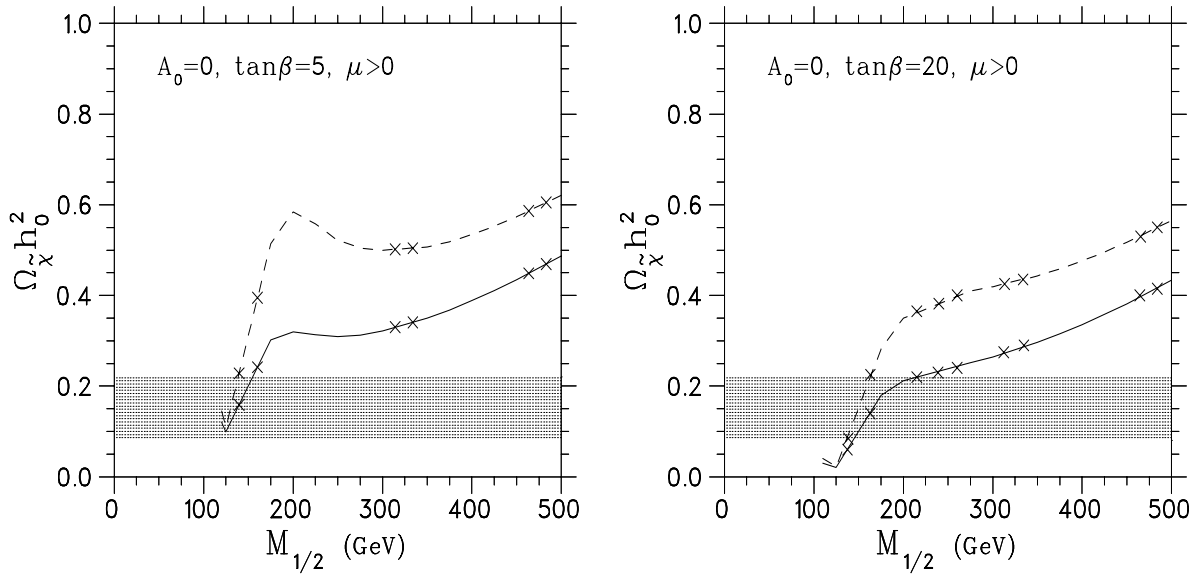


Figure 3: The relic density as function of $M_{1/2}$ for fixed values of A_0 , $\tan\beta$ shown in the figure. The solid and dashed lines correspond to values $m_0 = 150$ GeV and 200 GeV respectively.

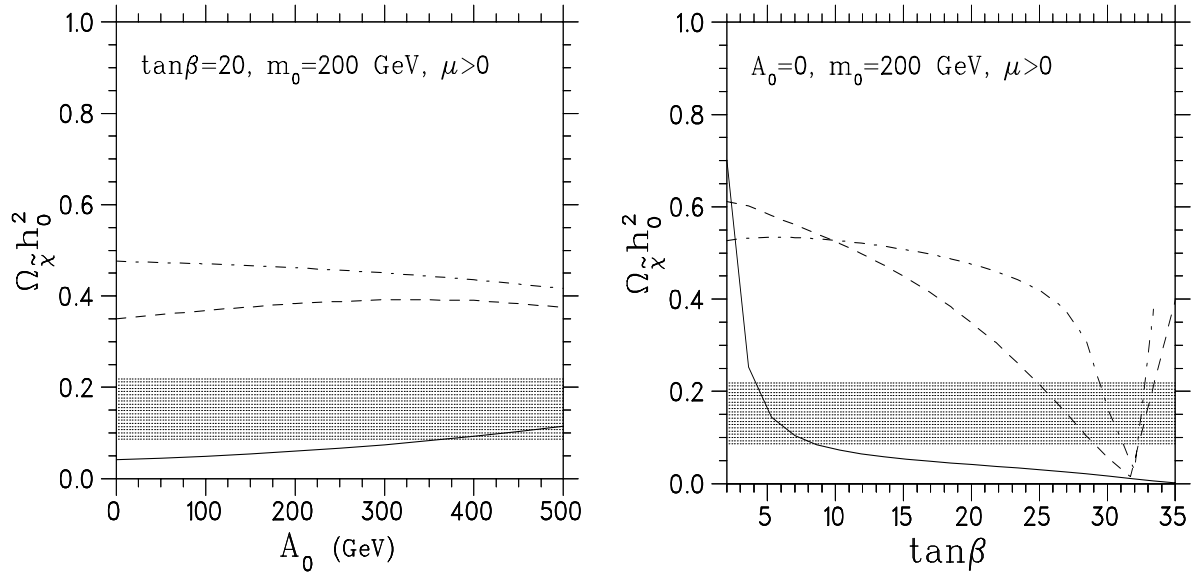


Figure 4: The relic density as function of A_0 and $\tan\beta$ for fixed values of the remaining parameters. The solid, dashed and dot-dashed lines correspond to $M_{1/2} = 120, 200$ and 400 GeV respectively.

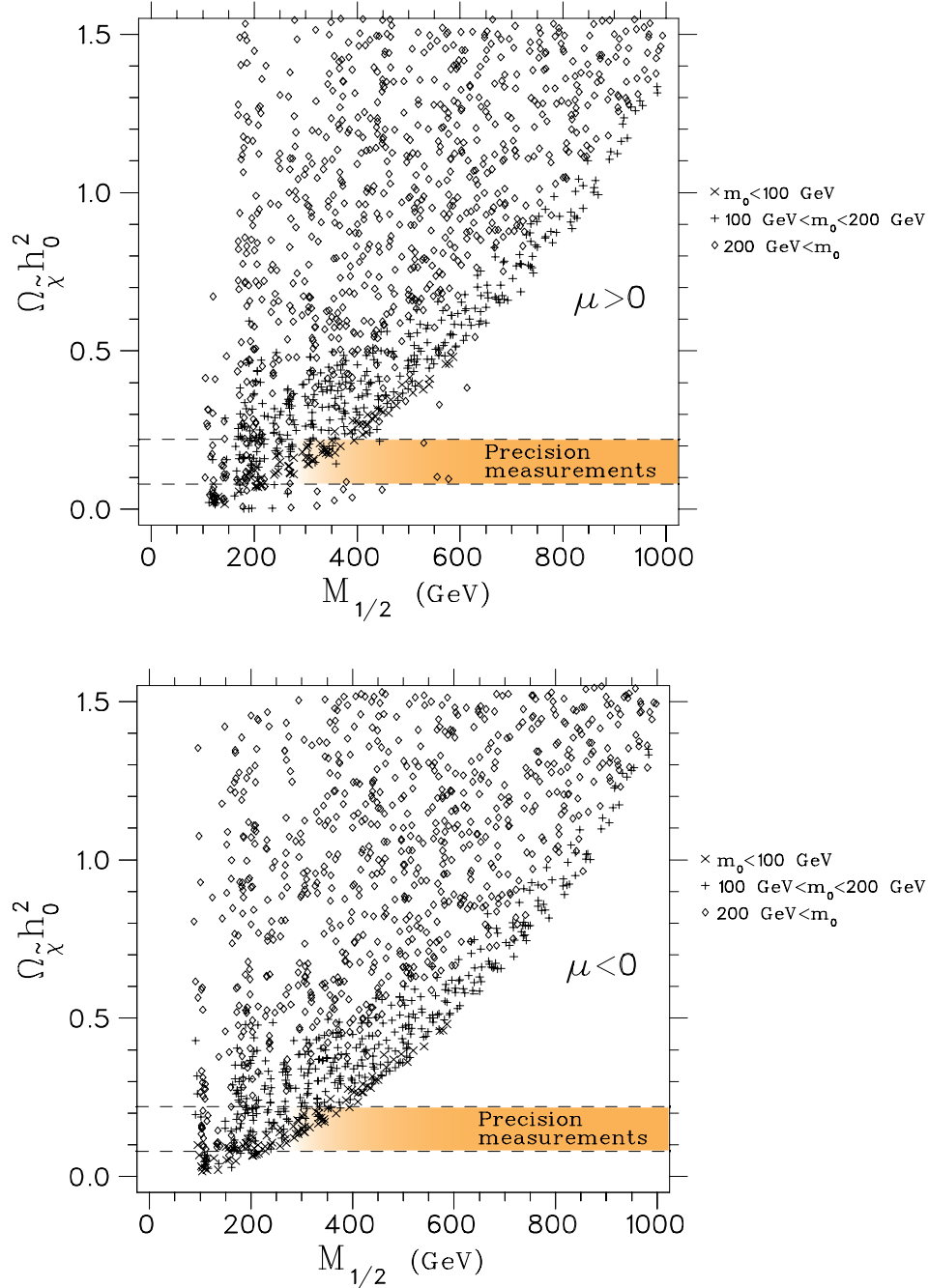


Figure 5: Scattered plot of the relic density versus $M_{1/2}$ from a sample of 4000 random points in the parameter space. Only the points with $\Omega_{\tilde{\chi}} h_0^2$ less than 1.5 are shown. The grey tone region within the cosmologically allowed stripe designates the region which agrees with EW precision data.